CLASSIFYING SUPERNOVA NEUTRINO EVENTS IN LIQUID ARGON TIME PROJECTION CHAMBER USING CONVOLUTIONAL NEURAL NETWORKS

Peijing Pang
Department of Physics and Astronomy
University College London
London, United Kingdom
zcapppa@ucl.ac.uk

ABSTRACT

This work investigates the ability of Convolutional Neural Networks (CNNs) in the classification of supernova neutrino events from background noise within Liquid-Argon Time Projection Chambers (LArTPCs), for electronic and radioactive noise environments. Using neutrino event image data and employing binary classification, the study assesses the performance of CNNs under varying noise levels. Classifier `C2` maintains high test accuracies against electronic noise, successfully classifying the majority of events. For radiological background, challenges arise with elongated noise blobs, particularly those exceeding 10 MeV in height, which correspond to the energy signatures from ^{36}Ar captures. The findings underscore the potential of CNNs in accurately classifying neutrino events in LArTPCs, offering promising implications for the development of early warning systems for supernova detection.

1 INTRODUCTION

SN 1987A was a type II supernova from the explosion of a blue supergiant, in a dwarf satellite galaxy of the Milky Way - the Large Magellanic Cloud (Utrobin, V. P. et al., 2015). Due to the low interaction rates, neutrinos produced by supernovae can escape more easily than light. Therefore, an early warning system for supernovae (Antonioli et al., 2004) can be developed by detecting supernova neutrinos efficiently.

Liquid-Argon Time Projection Chamber (LArTPC) (Rubbia, 1977) is a technology used commonly for neutrino detections in current and planned projects (MicroBooNE Collaboration, 2017; DUNE Collaboration, 2016). With an applied electric field across the chamber filled with liquid argon, events caused by incoming neutrinos produce charged particles which then ionises the argon. Electrons released from the argon atoms drift towards a collecting array of anode, where three-

Table 1: Meta Information Structure

Column	Description
0	Row number
1	Neutrino Energy (MeV)
2	Initial state particles (always 2)
3	Final state particles (varies)
4-8	Initial Particle 1: PDG code (Garren et al., 2024), Total Energy (MeV), p_x, p_y, p_z
9-13	Initial Particle 2: PDG code, Total Energy (MeV), p_x, p_y, p_z
14-18	Final Particle 1: PDG code, Total Energy (MeV), p_x, p_y, p_z
19-23	Final Particle 2: PDG code, Total Energy (MeV), p_x, p_y, p_z
⋮	Final Particle N: PDG code, Total Energy (MeV), p_x, p_y, p_z
59-63	Final Particle 10: PDG code, Total Energy (MeV), p_x, p_y, p_z

dimensional pictures of the events are reconstructed (Rubbia, 1977). The aim of this work is to apply machine learning algorithms in order to classify the neutrino events in LArTPCs.

For image classification, the network architecture, Convolutional Neural Networks (CNNs) are used. CNNs are feed-forward neural networks, which compute convolutions by sliding fixed 'filters' over the image (Kaplan, 2019). Machine learning algorithms with CNNs can learn patterns and features of the input images through training, thus obtaining the ability for classification.

2 Data Structure and Preparation

The LArTPC neutrino data for this study comprises a set of 100×100 pixel images, each consisting of a clean event, which displays the energy deposited in the chamber across a slice of space and time. Each image comes with its meta information, containing an array of 64 numbers for different purposes, as displayed in Table 1.

Given that the objective of the research is to identify these events, it is necessary to mix the neutrino images with empty images (off-event slices). To simulate the actual environment within the TPC, noise features will be generated and overlaid onto the images to recreate the conditions experienced in the TPC.

This work conducts the analysis in Python notebook. The neutrino images are labelled as '1', while the empty images as '0'. The empty images are generated with `NumPy` function `zeros`. The provided dataset of neutrino images is divided into two sets for the purposes of training and testing the algorithm, thus ensuring that the algorithm is not tested on images it has already seen. A training/testing dataset is then created by concatenating the neutrino and empty images, along with their labels. Next, the two types of images are mixed by assigning indices to the set and using `NumPy` function `random.permutation` to shuffle the set, so the algorithm does not learn any patterns.

2.1 LEVEL OF NOISE

The level of noise overlaid of this project needs to be considered by examining the scale of activated pixels in the neutrino images. It can be seen from Fig. 1 that the majority of activated pixels have a value below 20 MeV. The standard deviation of values σ_a is then calculated to be 5.6 MeV.

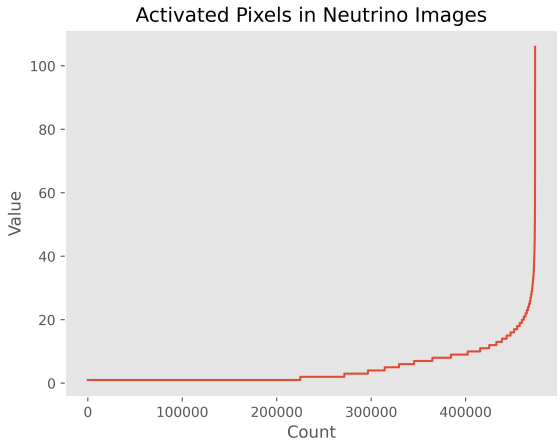

Figure 1: Values for all activates pixels in the given set of neutrino events.

3 BINARY CLASSIFIER – NETWORK STRUCTURE

The classifier algorithm for this work is binary. Being a CNN, a classifier in this project has a core of two convolutional layers, each followed by a max-pooling layer, as shown in Fig. 2. The first convolutional layer has 32 filters of size 3x3 and uses the `ReLU` activation function. Following each convolutional layer, a max-pooling layer of size 2x2 reduces the spatial dimensions of the output from the previous layer, helping to decrease the computational load and control overfitting by abstracting the features. In the end, the classifier uses the loss function binary cross entropy for training.

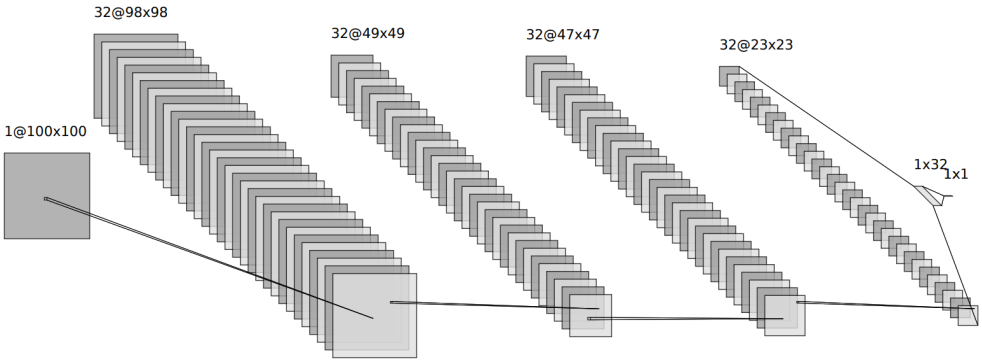

conv2d_input	input:	[(None, 100, 100, 1)]
InputLayer	output:	[(None, 100, 100, 1)]

conv2d	input:	(None, 100, 100, 1)
Conv2D	output:	(None, 98, 98, 32)

max_pooling2d	input:	(None, 98, 98, 32)
MaxPooling2D	output:	(None, 49, 49, 32)

conv2d_1	input:	(None, 49, 49, 32)
Conv2D	output:	(None, 47, 47, 32)

max_pooling2d_1	input:	(None, 47, 47, 32)
MaxPooling2D	output:	(None, 23, 23, 32)

flatten	input:	(None, 23, 23, 32)
Flatten	output:	(None, 16928)

dense	input:	(None, 16928)
Dense	output:	(None, 32)

dropout	input:	(None, 32)
Dropout	output:	(None, 32)

dense_1	input:	(None, 32)
Dense	output:	(None, 1)

Figure 2: Event classifier structure visualisation and layer details.

4 ELECTRONIC NOISE

4.1 SIMULATION

Noise from the electronics of the TPC are overlaid on the entire image by addition, as shown in Fig. 3, with value generated from a normal distribution, using `NumPy` function `random.normal`. A given level of noise is specified, which defines the standard deviation of the normal distribution, while the mean is set to 0.

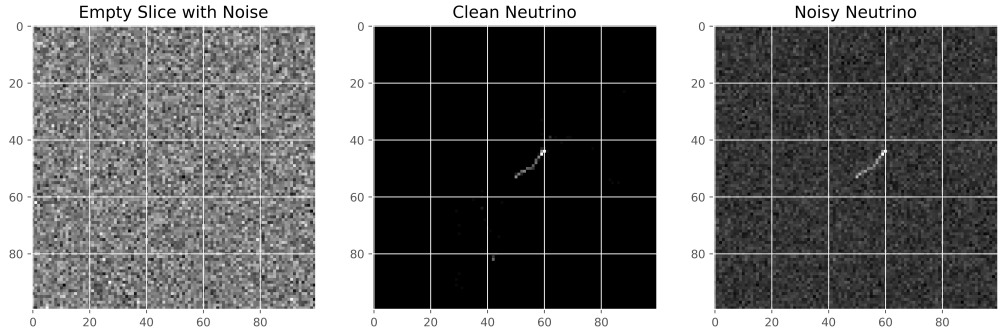

Figure 3: Examples of an empty image with electronic noise, a clean neutrino image, and a noisy neutrino image.

4.2 METHOD AND RESULT

First, neutrino events are kept clean and mixed with noisy empty images. A classifier `C0` is first trained on clean neutrino and noisy images and tested on testing datasets at different noise levels. The test accuracy is displayed in Fig. 4. Next, a new classifier `C1` is trained on noise level of σ_a. Repeating the same testing process, `C1` maintains its accuracy upon increasing noise level, as shown in Fig. 5. Its performance is then verified by evaluating the fractions of correctly classified images, as shown in Fig. 6.

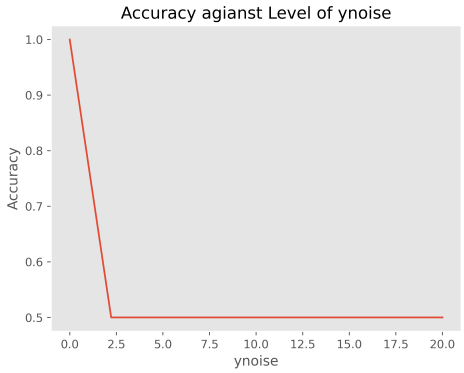

Figure 4: Test accuracy for `C0` which was trained on clean empty and neutrino images, classifying clean neutrinos. The accuracy approaches 0.5 at around half of σ_a.

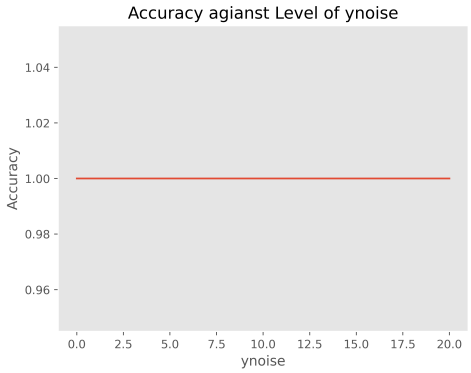

Figure 5: Test accuracy for `C1` which was trained on noisy empty and clean neutrino images, classifying clean neutrinos. Its performance is unaffected by noise level.

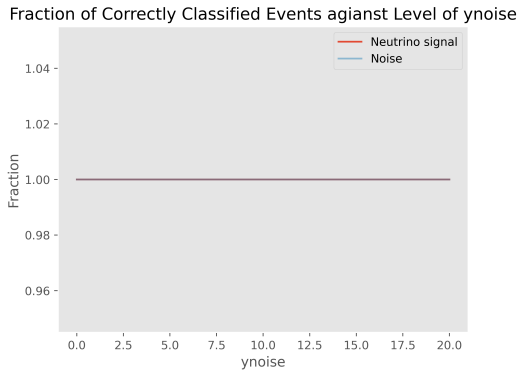

Figure 6: Fractions of correctly classified neutrino and noise images against noise level for `C1`. Both are unaffected.

The neutrino events are then overlaid with noise as well. `C1`'s test accuracy are displayed in Fig. 7. The classifier needs to be trained on noisy neutrinos, therefore, classifier `C2` is trained, with its test accuracy shown in Fig. 8. Further evaluation of `C2`'s performance is shown in Fig. 9.

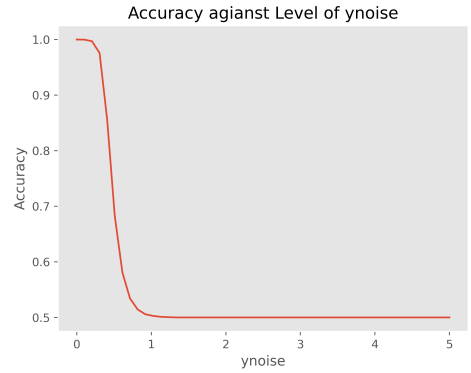

Figure 7: Test accuracy of `C1` on noisy neutrinos. Having not seen noisy neutrinos, the performance of `C1` tends towards random guessing immediately, at noise level of 0.5 MeV.

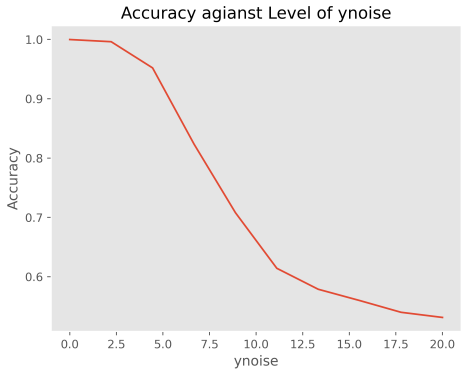

Figure 8: Test accuracy of `C2` which was trained on noisy neutrino and empty images.`C2`'s accuracy only begins to decrease at noise levels around σ_a, suggesting robustness against noise compared to `C1`.

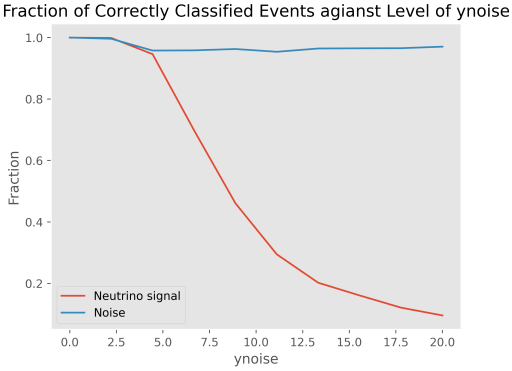

Figure 9: Fractions of correctly classified neutrino and noise images against noise level for `C2`. As the noise level escalates, `C2` increasingly fails to identify neutrino events, albeit without falsely recognising noise as neutrinos.

5 Radioactive Noise

5.1 Simulation

Inside the LArTPC, there also exists a radioactive background from decaying isotopes. The radioactive noises are simulated as a 3-dimensional Gaussian 'blob', which can be represented in a slice in x-y plane and another in x-z plane, as shown in Fig. 10.

The two blob slices are then overlaid on each image in the training/testing dataset, creating an otherwise pair of images. Examples of the images in the dataset for the radioactive noise are displayed in Fig. 11.

5.2 Method and Result

Similarly, a classifier `Cr0` is trained and tested on clean neutrinos mixed with empty slices. For this analysis, the test accuracy of `Cr0` is systematically evaluated across a range of noise blob dimensions. Both the width and height of the noise blob are varied within a defined range. This variation is implemented through nested for loops, which iterate over each combination of width

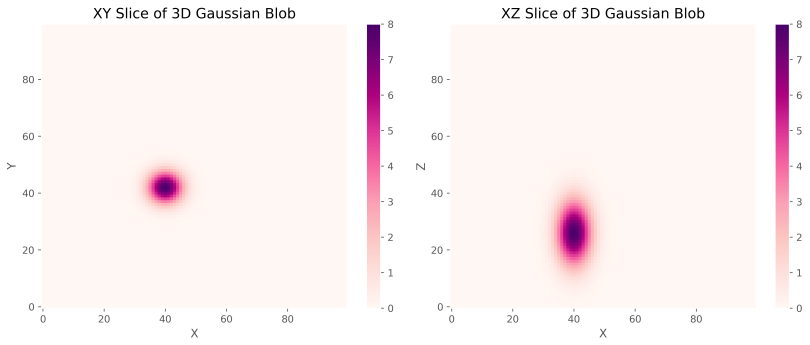

Figure 10: Slices of the same 3D Gaussian blob in the two planes. The width defines the spread of the blob in the x-y plane, the height defines the intensity and length in the x-z plane.

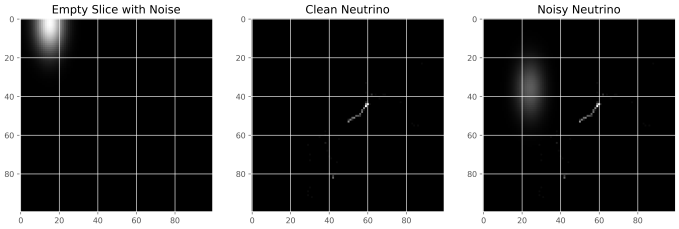

Figure 11: Examples for noisy empty images and noisy neutrino images, with blob of width 4 and height 8.

and height from 1 to 40. The corresponding test accuracies for each combination are calculated and stored in a two-dimensional array and visualised using `pcolormesh` from `Matplotlib` as shown in Fig. 12.

`Cr0` is then tested with noisy neutrinos. The result is displayed in Fig. 13, the accuracy quickly approaches 0.5 for random guessing. Three classifiers are subsequently trained, named `Cr1`, `Cr2` and `Cr3` on noisy neutrinos. The analysis is repeated for all three, as shown in Fig. 14.

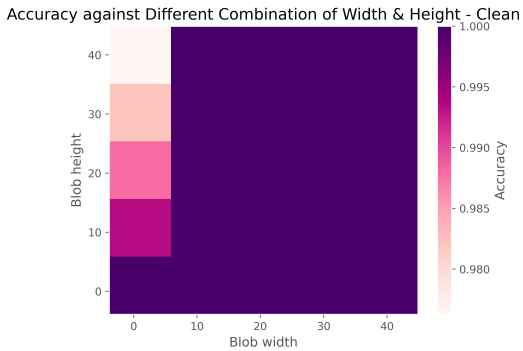

Figure 12: Test accuracy against width and height for `Cr0` with clean neutrinos. With clean neutrinos, the classifier only loses small accuracy for elongated blobs, with small widths and large heights.

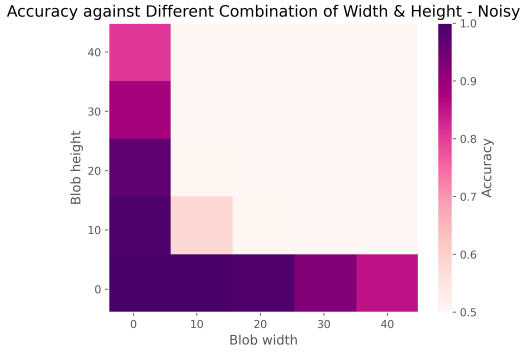

Figure 13: Test accuracy against width and height for `Cr0` with noisy neutrinos. Accuracy immediately drops to 0.5 when the width and height are increased.

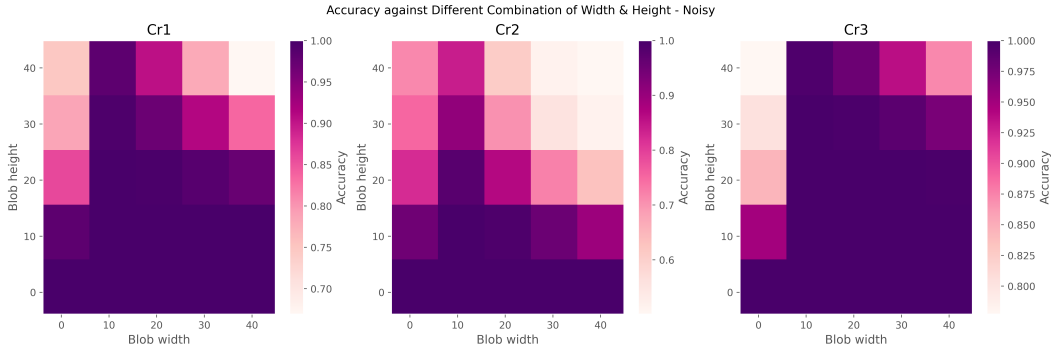

Figure 14: Test accuracy against width and height for `Cr1`, `Cr2` and `Cr3` with noisy neutrinos. `Cr1` was trained on width 5, height 20; `Cr2` was trained on width 10, height 5; `Cr3` was trained on width 15, height 15. They all obtain good accuracy for all combinations when the general level is low. All classifiers demonstrate good accuracy across the various combinations when the overall noise level remains low. However, as the noise level increases, particularly when it masks the neutrino signals, a noticeable decline in accuracy is observed. Notably, all classifiers encounter challenges where the noise blobs are elongated with large heights and low widths.

5.2.1 Misclassified Images

Further investigation is subsequently made into which images are misclassified with radioactive noise. New training/testing datasets are created with overlaid noise blobs of random widths and heights. Classifier `CrR` is created, trained, and tested. The misclassified neutrino and empty images are found and investigated. With a high test accuracy of 0.9974, `CR` is tested repeatedly, and all the misclassified images are collected. For this task, meta information is incorporated within the testing dataset to facilitate analysis of the types of events that are frequently misclassified.

The neutrino images are displayed in Fig. 15, and empty images in Fig. 16. Viewing the meta information for each misclassified neutrino image, excluding the covered neutrino events, all others are those from low-energy neutrinos with noise blobs of small widths and heights. The misclassified neutrino events have a typical energy of $\sim$10 MeV. For empty images, despite the large noise blobs which cause confusion, the elongated blobs are frequently identified as events, coinciding with the result from Fig. 14.

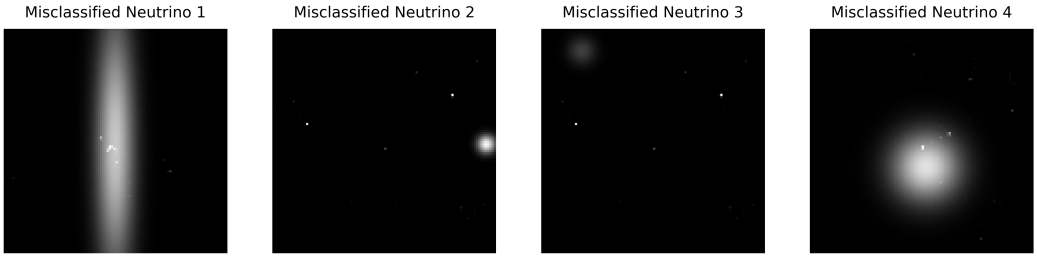

Figure 15: Misclassified neutrino images for `CrR`. The noise blob obscures the first and fourth events, making them hard to distinguish. The second and third events have energies similar to the blob, which leads to confusion.

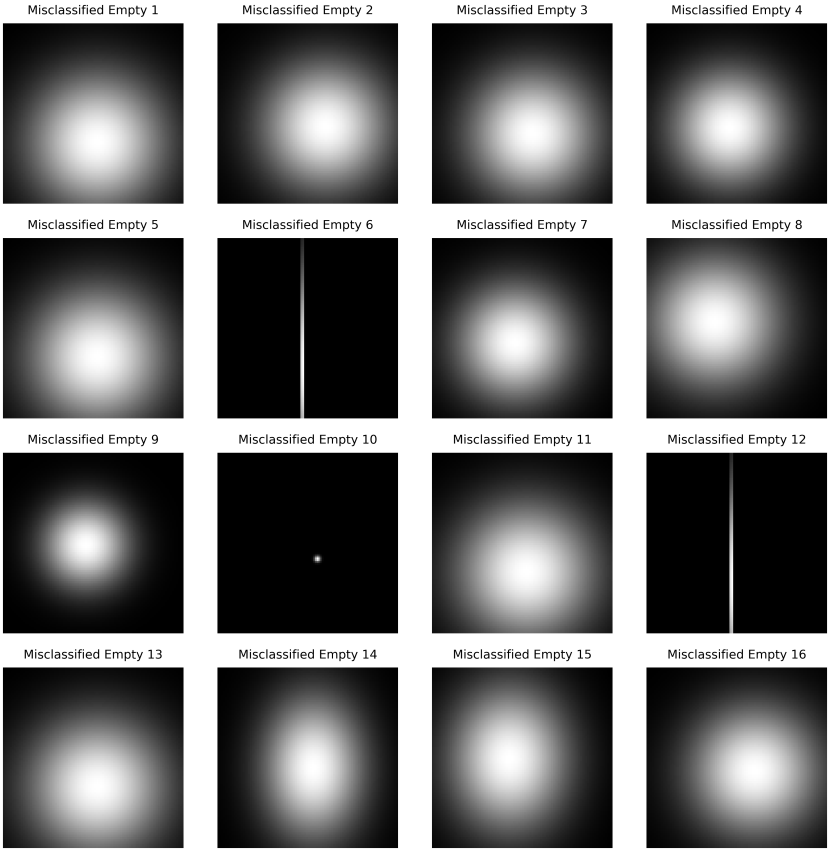

Figure 16: Sixteen randomly selected misclassified empty images for `CrR`. Despite the high energy blobs, `CrR` also failed to classify elongated blobs. Images 5 and 12 are x-z plane slices, while image 10 is an x-y plane slice.

6 Conclusion

Overall, this work demonstrates the ability of CNNs in distinguishing between neutrino events and empty slices amidst both electronic and radioactive noise within LArTPCs.

A typical level of electronic noise for LArTPCs is 7.3 MeV (Radeka, 1977). Compared to Fig. 8 and Fig. 9, `C2` at this level has a test accuracy of above 0.8, with $\sim$95% of neutrino and $\sim$70% of empty images correctly classified.

For the radioactive noise analysis, all `Cr` classifiers experienced difficulties for elongated noise blobs of heights $\geq$10 MeV. This specific threshold aligns with the energy profiles of ^{36}Ar captures, known to generate gamma cascades around 9 MeV (Bezerra et al., 2023), indicating that radiological background substantially impacts the algorithm's effectiveness.

In summary, the findings affirm the potential of deploying CNNs for the precise classification of neutrino events in LArTPCs. This capability paves the way for their application in early warning systems for supernovae detection, marking a significant advancement in the field.

REFERENCES

Pietro Antonioli, Richard Tresch Fienberg, Fabrice Fleurot, Yoshiyuki Fukuda, Walter Fulgione, Alec Habig, Jaret Heise, Arthur B McDonald, Corrinne Mills, Toshio Namba, Leif J Robinson, Kate Scholberg, Michael Schwendener, Roger W Sinnott, Blake Stacey, Yoichiro Suzuki, Réda Tafirout, Carlo Vigorito, Brett Viren, Clarence Virtue, and Antonino Zichichi. Snews: the supernova early warning system. *New Journal of Physics*, 6:114–114, September 2004. ISSN 1367-2630. doi: 10.1088/1367-2630/6/1/114. URL `http://dx.doi.org/10.1088/1367-2630/6/1/114`.

T Bezerra, A Borkum, E Church, Z Djurcic, J Genovesi, J Haiston, C M Jackson, I Lazanu, B Monreal, S Munson, C Ortiz, M Parvu, S J M Peeters, D Pershey, S S Poudel, J Reichenbacher, R Saldanha, K Scholberg, G Sinev, S Westerdale, and J Zennamo. Large low background kton-scale liquid argon time projection chambers. *Journal of Physics G: Nuclear and Particle Physics*, 50(6):060502, may 2023. doi: 10.1088/1361-6471/acc394. URL `https://dx.doi.org/10.1088/1361-6471/acc394`.

DUNE Collaboration. Long-baseline neutrino facility (lbnf) and deep underground neutrino experiment (dune) conceptual design report volume 1: The lbnf and dune projects, 2016.

L. Garren, C.-J. Lin, Sergio Navas, P. Richardson, T. Sjóstrand, et al. Monte carlo particle numbering scheme. 2024.

Jared Kaplan. Notes on contemporary machine learning for physicists. 2019. URL `https://api.semanticscholar.org/CorpusID:121204748`.

MicroBooNE Collaboration. Design and construction of the microboone detector. *Journal of Instrumentation*, 12(02):P02017–P02017, February 2017. ISSN 1748-0221. doi: 10.1088/1748-0221/12/02/p02017. URL `http://dx.doi.org/10.1088/1748-0221/12/02/P02017`.

V. Radeka. High resolution liquid argon total-absorption detectors: Electronic noise and electrode configuration. *IEEE Transactions on Nuclear Science*, 24(1):293–298, 1977. doi: 10.1109/TNS.1977.4328692.

Carlo Rubbia. The liquid-argon time projection chamber: a new concept for neutrino detectors. Technical report, CERN, Geneva, 1977. URL `https://cds.cern.ch/record/117852`.

Utrobin, V. P., Wongwathanarat, A., Janka, H.-Th., and Müller, E. Supernova 1987a: neutrino-driven explosions in three dimensions and light curves. *AA*, 581:A40, 2015. doi: 10.1051/0004-6361/201425513. URL `https://doi.org/10.1051/0004-6361/201425513`.